Higgs quadruplet impact on W mass shift, dark matter, and LHC signatures

Talal Ahmed Chowdhury,[1] Kareem Ezzat,[2,3] Shaaban Khalil,[3] Ernest Ma,[4] and Dibyendu Nanda[5]

[1]*Department of Physics, University of Dhaka, P.O. Box 1000, Dhaka, Bangladesh*
[2]*Department of Mathematics, Faculty of Science, Ain Shams University, Cairo 11566, Egypt*
[3]*Center for Fundamental Physics, Zewail City of Science and Technology, Sheikh Zayed, 12588, Giza, Egypt*
[4]*Department of Physics and Astronomy, University of California, Riverside, California 92521, USA*
[5]*School of Physics, Korea Institute for Advanced Study, Seoul 02455, South Korea*

(Received 19 January 2024; accepted 26 March 2024; published 22 April 2024)

The addition of a Higgs quadruplet to the standard model (SM) of quarks and leptons would shift the W-boson mass upward. It could also facilitate the production of dark matter through the conventional thermal freeze-out scenario via Yukawa interaction with the Higgs quadruplet or freeze-in production from the decay of SM Higgs. We investigate the same-sign lepton smoking gun signature of the double-charged scalar component of the quadruplet Higgs at the LHC.

DOI: 10.1103/PhysRevD.109.075039

The Standard Model (SM) of quarks and leptons has one Higgs doublet $\Phi = (\phi^+, \phi^0)$. When the gauge symmetry $SU(2)_L \times U(1)_Y$ undergoes spontaneous symmetry breaking due to $\langle \phi^0 \rangle = v_0$, a well-established tree-level condition emerges; $\rho = M_W^2/M_Z^2 \cos^2\theta_W = 1$. The recent measurement of the W-boson's mass by the CDF experiment is given by $m_W^{\rm CDF} = 80.4335 \pm 0.094$ GeV [1], which shows 7σ deviation from the SM prediction; $m_W^{\rm SM} = 80.357 \pm 0.006$ GeV. This has prompted theorists to speculate about potential new physics contributing to this unexpected increase in the W-boson's mass.

If an additional Higgs multiplet with an isospin I is introduced to the SM, the vacuum expectation value v_1 of its neutral component, having third component of isospin I_3, contributes $2(g^2/\cos^2\theta_W) I_3^2 v_1^2$ to M_Z^2 and $g^2[I(I+1) - I_3^2] v_1^2$ to M_W^2. As a result, ρ deviates from unity except for certain specific values of I and I_3. Notably, the ρ parameter derived from electroweak global fits is $\rho = 1.0002 \pm 0.0009$ [2]. Therefore, this leads to stringent constraints on the value of v_1.

In this letter, we study the effect of adding a Higgs quadruplet $\zeta = (\zeta^{++}, \zeta^+, \zeta^0, \zeta^-)$ to the SM. The motivation for extending the SM with a Higgs quadruplet primarily stems from the quest to resolve the neutrino mass problem. The contribution of $\langle \zeta^0 \rangle = v_\zeta$ to M_W^2 is $7 g^2 v_\zeta^2/2$, and that to M_Z^2 is $g^2 v_\zeta^2/2\cos^2\theta_W$. This could then explain the W-mass shift, in agreement with the recent precision measurement [1]. Whereas ζ is necessary for the quintuplet neutrino seesaw mechanism [3,4], it may also be the connector in type III seesaw [5]. In our model, another use of ζ is proposed, as the connector to the dark sector consisting of a neutral Majorana fermion singlet N and a Dirac fermion quadruplet $\Sigma = (\Sigma^{++}, \Sigma^+, \Sigma^0, \Sigma^-)$.

Consider the Higgs quadruplet ζ. It interacts with (W^+, W^0, W^-) and the $U(1)_Y$ gauge boson B according to $|(\partial_\mu - ig\mathcal{W}_\mu^{(4)} - i(g'/2)B_\mu)\zeta|^2$, where

$$\mathcal{W}^{(4)} = \begin{pmatrix} (3/2)W^0 & \sqrt{3/2}W^+ & 0 & 0 \\ \sqrt{3/2}W^- & (1/2)W^0 & \sqrt{2}W^+ & 0 \\ 0 & \sqrt{2}W^- & -(1/2)W^0 & \sqrt{3/2}W^+ \\ 0 & 0 & \sqrt{3/2}W^- & -(3/2)W^0 \end{pmatrix}. \tag{1}$$

For the fermion quadruplet Σ, the corresponding interaction is $\bar{\Sigma}\gamma^\mu(\partial_\mu - ig\mathcal{W}_\mu^{(4)} - i(g'/2)B_\mu)\Sigma$. We assume that Σ is odd under a dark Z_2 symmetry together with a neutral singlet fermion N. Hence $\zeta^\dagger \Sigma N$ is allowed and ζ becomes the connection between the SM and the dark sector. The Higgs potential consisting of Φ and ζ is given by [4]

$$V = -\mu_1^2\Phi^\dagger\Phi + \mu_2^2\zeta^\dagger\zeta + \frac{1}{2}\lambda_1(\Phi^\dagger\Phi)^2 + \frac{1}{2}\lambda_2(\zeta^\dagger\zeta)^2 + \frac{1}{2}\lambda_2'[\zeta^\dagger\zeta]_i[\zeta^\dagger\zeta]_i + \lambda_3(\Phi^\dagger\Phi)(\zeta^\dagger\zeta) + \lambda_3'[\Phi^\dagger\Phi]_i[\zeta^\dagger\zeta]_i + \left\{\frac{1}{2}\lambda_3''[\Phi^\dagger\zeta]_i[\Phi^\dagger\zeta]_i + \text{H.c.}\right\} - \left\{\frac{1}{3}\lambda_4[\zeta^\dagger\Phi]_i[\Phi^\dagger\Phi]_i + \text{H.c.}\right\} - \left\{\frac{1}{3}\lambda_5[\Phi^\dagger\zeta^\dagger]_i[\zeta\zeta]_i + \text{H.c.}\right\}, \tag{2}$$

where the sum over $i = 1, 2, 3$ represents the components of the tensor product of the scalar fields. There are in principle four quartic terms of the type $(\zeta^\dagger\zeta)(\zeta^\dagger\zeta)$, corresponding to the pairings 1×1, 3×3, 5×5, and 7×7, where 1×1 indicates the multiplication between singlet components of each product, whereas 3×3 represents the multiplication between triplet components, and so on. However, the 5×5 term is proportional to 1×1. The sum of 3×3 and 7×7 is also proportional to 1×1. Hence, there are only two independent terms. As for the terms mixing ζ with Φ, $(\Phi^\dagger\Phi)(\zeta^\dagger\zeta)$ has two terms, whereas $(\Phi^\dagger\zeta)(\Phi^\dagger\zeta)$, $(\zeta^\dagger\Phi)(\Phi^\dagger\Phi)$, $(\Phi^\dagger\zeta^\dagger)(\zeta\zeta)$, each has just one term. Now, the different terms of the scalar potential can be expressed by using the tensorial notation of ζ as follows:

$$[\zeta^\dagger\zeta]_i[\zeta^\dagger\zeta]_i = [3|\zeta^{++}|^2 + |\zeta^+|^2 - |\zeta^0|^2 - 3|\zeta^-|^2]^2 + 4|\sqrt{3}\zeta^{++}\overline{\zeta^+} + 2\zeta^+\overline{\zeta^0} + \sqrt{3}\zeta^0\overline{\zeta^-}|^2, \tag{3}$$

$$[\Phi^\dagger\Phi]_i[\zeta^\dagger\zeta]_i = [|\phi^+|^2 - |\phi^0|^2][3|\zeta^{++}|^2 + |\zeta^+|^2 - |\zeta^0|^2 - 3|\zeta^-|^2] + \{2\phi^+\overline{\phi^0}[\sqrt{3}\zeta^+\overline{\zeta^{++}} + 2\zeta^0\overline{\zeta^+} + \sqrt{3}\zeta^-\overline{\zeta^0}] + \text{H.c.}\}, \tag{4}$$

$$[\Phi^\dagger\zeta]_i[\Phi^\dagger\zeta]_i = (\overline{\phi^0}\zeta^0 + \phi^-\zeta^+)^2 - (\overline{\phi^0}\zeta^+ + \sqrt{3}\phi^-\zeta^{++})(\sqrt{3}\overline{\phi^0}\zeta^- + \phi^-\zeta^0), \tag{5}$$

$$[\zeta^\dagger\Phi]_i[\Phi^\dagger\Phi]_i = [\overline{\zeta^0}\phi^0 + \overline{\zeta^+}\phi^+][|\phi^0|^2 - |\phi^+|^2] + [\overline{\zeta^+}\phi^0 + \sqrt{3}\overline{\zeta^{++}}\phi^+]\phi^+\overline{\phi^0} - [\sqrt{3}\overline{\zeta^-}\phi^0 + \overline{\zeta^0}\phi^+]\phi^0\phi^-, \tag{6}$$

$$[\Phi^\dagger\zeta^\dagger]_i[\zeta\zeta]_i = (\overline{\phi^0}\,\overline{\zeta^0} - \sqrt{3}\phi^-\overline{\zeta^-})(\zeta^0\zeta^0 - \sqrt{3}\zeta^+\zeta^-) + (\overline{\phi^0}\,\overline{\zeta^+} - \phi^-\overline{\zeta^0})(\zeta^+\zeta^0 - 3\zeta^{++}\zeta^-) + (\sqrt{3}\overline{\phi^0}\,\overline{\zeta^{++}} - \phi^-\overline{\zeta^+})(\zeta^+\zeta^+ - \sqrt{3}\zeta^{++}\zeta^0). \tag{7}$$

Let $\langle\phi^0\rangle = v_0$ and $\langle\zeta^0\rangle = v_\zeta$, then the minimum of V is determined by $0 = v_0[-\mu_1^2 + \lambda_1 v_0^2 + (\lambda_3 + \lambda_3' + \lambda_3'')v_\zeta^2 - \lambda_4 v_0 v_\zeta] - \frac{1}{3}\lambda_5 v_\zeta^3$ and $0 = v_\zeta[\mu_2^2 + (\lambda_2 + \lambda_2')v_\zeta^2 + (\lambda_3 + \lambda_3' + \lambda_3'')v_0^2 - \lambda_5 v_0 v_\zeta] - \frac{1}{3}\lambda_4 v_0^3$. For positive and large μ_2^2, $v_\zeta \simeq \lambda_4 v_0^3/3\mu_2^2 \ll v_0$. This is the analog of the scalar seesaw studied previously in Refs. [6,7]. Let $h = \sqrt{2}\text{Re}(\phi^0)$ and $H = \sqrt{2}\text{Re}(\zeta^0)$, then their 2×2 mass-squared matrix is

$$\mathcal{M}_{hH}^2 = \begin{pmatrix} 2\lambda_1 v_0^2 - \lambda_4 v_0 v_\zeta + \lambda_5 v_\zeta^3/3v_0 & -\lambda_4 v_0^2 + 2(\lambda_3 + \lambda_3' + \lambda_3'')v_\zeta v_0 - \lambda_5 v_\zeta^2 \\ -\lambda_4 v_0^2 + 2(\lambda_3 + \lambda_3' + \lambda_3'')v_\zeta v_0 - \lambda_5 v_\zeta^2 & \lambda_4 v_0^3/3v_\zeta - \lambda_5 v_0 v_\zeta + 2(\lambda_2 + \lambda_2')v_\zeta^2 \end{pmatrix}. \tag{8}$$

The linear combination proportional to $v_0\text{Im}(\phi^0) + v_\zeta\text{Im}(\zeta^0)$ becomes the Goldstone boson for Z whereas its orthogonal combination has mass-squared $= (\lambda_4 v_0/3v_\zeta + \lambda_5 v_\zeta/3v_0)(v_0^2 + v_\zeta^2)$. The 3×3 mass-squared matrix spanning $(\phi^+, \zeta^+, \overline{\zeta^-})$ is

$$\mathcal{M}_+^2 = \begin{pmatrix} -2\lambda_3' v_\zeta^2 + 7\lambda_4 v_0 v_\zeta/3 & 4\lambda_3' v_0 v_\zeta - 2\lambda_4 v_0^2/3 & 2\sqrt{3}\lambda_3' v_0 v_\zeta + \lambda_4 v_0^2/\sqrt{3} \\ 4\lambda_3' v_0 v_\zeta - 2\lambda_4 v_0^2/3 & 6\lambda_2' v_\zeta^2 - 2\lambda_3' v_0^2 + \lambda_4 v_0^3/3v_\zeta & 4\sqrt{3}\lambda_2' v_\zeta^2 \\ 2\sqrt{3}\lambda_3' v_0 v_\zeta + \lambda_4 v_0^2/\sqrt{3} & 4\sqrt{3}\lambda_2' v_\zeta^2 & 8\lambda_2' v_\zeta^2 + 2\lambda_3' v_0^2 + \lambda_4 v_0^3/3v_\zeta \end{pmatrix} + \begin{pmatrix} -\lambda_3'' v_\zeta^2 + \lambda_5 v_\zeta^3/3v_0 & \lambda_3'' v_\zeta v_0/2 + \lambda_5 v_\zeta^2/3 & \lambda_5 v_\zeta^2/\sqrt{3} \\ \lambda_3'' v_\zeta v_0/2 + \lambda_5 v_\zeta^2/3 & -\lambda_3'' v_0^2 + \lambda_5 v_\zeta v_0/3 & -\sqrt{3}\lambda_3'' v_0^2/2 + \lambda_5 v_\zeta v_0/\sqrt{3} \\ \lambda_5 v_\zeta^2/\sqrt{3} & -\sqrt{3}\lambda_3'' v_0^2/2 + \lambda_5 v_\zeta v_0/\sqrt{3} & -\lambda_3'' v_0^2 + \lambda_5 v_\zeta v_0 \end{pmatrix}. \tag{9}$$

The linear combination proportional to $v_0\phi^+ + 2v_\zeta\zeta^+ - \sqrt{3}v_\zeta\zeta^-$ becomes the Goldstone boson for W^+ whereas the other two orthogonal combinations have mass-squared $= \lambda_4 v_0^3/3v_\zeta - \lambda_3'' v_0^2 \pm \sqrt{4(\lambda_3' v_0^2)^2 + 3(\lambda_3'' v_0^2)^2}/4$, neglecting terms of order $v_0 v_\zeta$ and smaller. The doubly charged scalar boson ζ^{++} has mass-squared $= \lambda_4 v_0^3/3v_\zeta - 4\lambda_3' v_0^2 - \lambda_3'' v_0^2 + 3\lambda_5 v_0 v_\zeta - 4\lambda_2' v_\zeta^2$. The other relevant renormalizable interactions can be written as

$$\mathcal{L}_{\rm Yuk} = i\bar{\Sigma}\bar{\sigma}^\mu D_\mu \Sigma + i\bar{N}\gamma^\mu \partial_\mu N + [y_N \zeta^\dagger \bar{N}\Sigma + M_\Sigma \bar{\Sigma}\Sigma + M_N \bar{N}N + \text{H.c.}]. \tag{10}$$

Let us now discuss the impact of our model in light of the CDF Collaboration measurement of the W-boson mass $M_W = 80433.5 \pm 9.4$ MeV [1] collected at the CDF-II detector of Fermilab Tevatron collider. The recently measured value of W-mass has a 7σ departure from the SM expectation ($M_W = 80357 \pm 6$ MeV). This has led to various different proposals on the feasible implications and interpretations related to electroweak precision parameters [8–11], beyond the Standard Model (BSM) physics like DM [12–17], additional scalar fields [18–29], effective field theory [30,31], supersymmetry [32–36], and several others [37–50]. We study the fit to the new measurement [1] of the W-boson mass, using newly added quadruplet ζ. The new physics contributions to W-boson mass anomaly can be parametrized in terms of the oblique parameters S, T, and U [51,52]. Considering the U parameter to be vanquished, any BSM physics contribution to W-boson mass can be parametrized in terms of S and T parameters. Taking the fine-structure constant α, the Fermi constant G_F, and Z boson mass M_Z as input parameters, the fitting of S and T parameters in view of the recent W-mass anomaly has been discussed in [31]. It is very important to note that, a change in the oblique parameters due to BSM physics will also change the precisely measured weak mixing angle θ_W. The $\sin^2_{\theta_W}(m_Z)_{\overline{\rm MS}}$ and the mass of W boson m_W can be expressed in terms of S and T parameters as [53]

$$M_W = 80.357\ \text{GeV}(1 - 0.0036S + 0.0056\,T),$$
$$\sin^2_{\theta_W}(m_Z)_{\overline{\rm MS}} = 0.23124(1 - 0.0157S + 0.0112\,T). \tag{11}$$

From the above two equations, it can be inferred that the compatibility of newly measurement of W-boson mass with the θ_W requires both S and T parameters to be nonzero, also seen from the fits shown in [31]. However, in the case of a scalar quadruplet ζ with hypercharge $1/2$, we will get a correction to the T parameter only as also shown in [9]. To take into account the enhanced W-boson mass, the required limit on the T parameter is $T = 0.17 \pm 0.020889$.

However, following Eq. (11), any change in the T parameter with $S = 0$ will put the weak mixing angle $\sin^2\theta_W$ in tension with the LEP data. The above-mentioned range of T would imply that $\sin^2\theta_W$ should lie in between 0.230746–0.230854. An additional contribution to S and T parameters would be required to reduce this tension. The T parameter will get a new contribution at tree level from the vacuum expectation value of $\zeta(v_\zeta)$ and can be written as $T = 6v_\zeta^2/\alpha v^2$ [9,54,55]. This can fit the M_W anomaly for $v_\zeta \approx 3$ GeV as shown in the left panel of Fig. 1. As v_ζ can be presented in terms of the bare mass term of ζ (μ_2) and the quartic coupling λ_4 as they are related via $\mu_2 \approx (\lambda_4 v^3/3v_\zeta)^{1/2}$, the corresponding constraints on v_ζ can also be translated in the μ_2-λ_4 plane, as shown in the right panel of Fig. 1. Importantly, λ_4 will also decide the mass of the doubly charged scalar ζ^{++} and we have discussed the impact of ζ^{++} in collider in the later part of this letter.

As mentioned above, the dark fermions N and $\Sigma = (\Sigma^{++}, \Sigma^+, \Sigma^0, \Sigma^-)$ are connected to the SM through ζ with the Yukawa coupling $y_N \zeta^\dagger \Sigma_L N_L$ + H. c. and the presence of an unbroken $\mathcal{Z}_2$ symmetry ensures the stability of either N or the neutral component of Σ to be a viable dark matter candidate of the model. As both ζ and Σ are charged under SM gauge symmetry, they can be thermalized with the SM bath through their gauge interactions.

Assuming N is lighter than Σ, N also can be thermally produced in the early Universe for a sizable y_N and eventually freezes out when its interaction rate drops below the expansion rate of the Universe. Assuming, ζ is lighter than the dark matter N, it can dominantly annihilate into the pair of ζ particles via the Yukawa interaction shown in Eq. (10). There can also be significant contributions from the coannihilation with different components of Σ. The dominant annihilation and coannihilation channels of N for different final states are shown in Fig. 2. As a result, the important parameters which can affect the relic abundance are the dark matter mass (M_N), the Yukawa coupling (y_N), and the mass splitting between Σ and N which is defined as $\Delta M = M_{\Sigma_i} - M_N$.

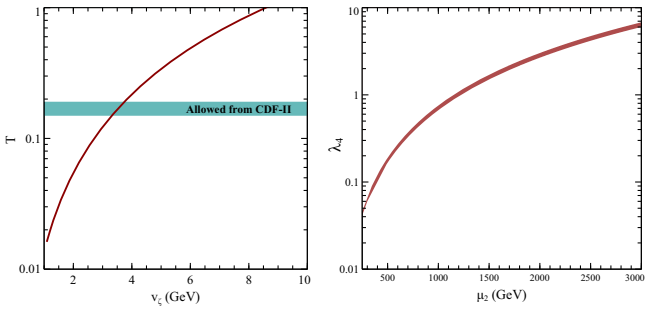

FIG. 1. The allowed values of v_ζ and the parameter space in the μ_2-λ_4 plane from the M_W anomaly.

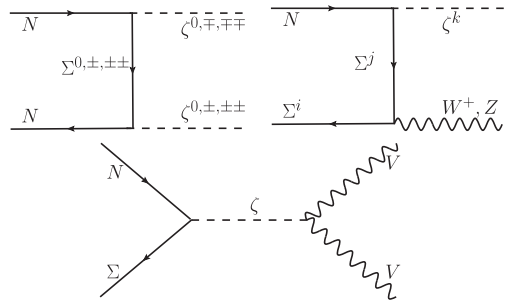

FIG. 2. Dominant annihilation and coannihilation channels of dark matter.

In Fig. 3, we have shown the allowed parameter space in M_N-ΔM plane as the variation of y_N is shown through the color code. It is important to note that the relic density can only be satisfied for larger mass splitting ΔM. For smaller mass splitting there can be huge coannihilation which suppresses the relic abundance which also sets a correlation with the Yukawa coupling y_N. The smaller the mass splitting stronger the coannihilation and one needs to reduce the Yukawa coupling to reduce the cross section.

Another interesting dark matter phenomenology can arise in the case of tiny Yukawa coupling (y_N). This can lead to the nonthermal production of dark matter. For tiny y_N, dark matter can be directly produced from the direct decay of SM Higgs. The 3×3 mass matrix spanning $(N_L, \Sigma_L^0, \overline{\Sigma_R^0})$ is then,

$$\mathcal{M}_{N\Sigma} = \begin{pmatrix} m_N & y_N v_\zeta & 0 \\ y_N v_\zeta & 0 & m_\Sigma \\ 0 & m_\Sigma & 0 \end{pmatrix}. \tag{12}$$

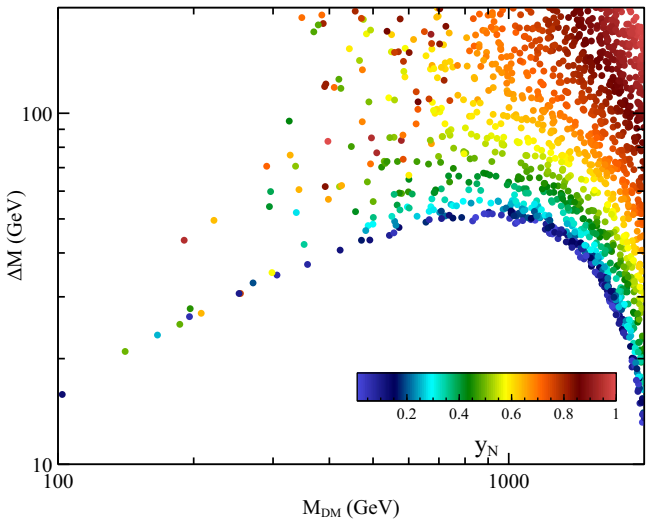

FIG. 3. The allowed parameter space in ΔM-M_N plane from the relic density constraints where the color code represents the variation of the Yukawa coupling y_N.

Assuming that m_N is of order GeV and m_Σ is very much heavier, the $N - \Sigma$ mixing is $y_N v_\zeta / m_\Sigma$. Consider now the decay of the SM Higgs h to NN. It does so first through $h - H$ mixing which is roughly $v_\zeta / 3v_0$, then through $N - \Sigma$ mixing as just noted. The effective coupling is

$$f_h = \left(\frac{v_\zeta}{3v_0}\right)\left(\frac{y_N}{\sqrt{2}}\right)\left(\frac{y_N v_\zeta}{m_\Sigma}\right). \tag{13}$$

The decay rate of h to $NN + \bar{N}\bar{N}$ is [56]

$$\Gamma_h = \frac{f_h^2 m_h}{8\pi}\sqrt{1-4x^2}(1-2x^2), \tag{14}$$

where $x = m_N/m_h$. The correct dark matter relic abundance is obtained [57] if $f_h \sim 10^{-12} x^{-1/2}$, provided that the reheat temperature of the Universe is above m_h but well-below m_H and m_Σ. For $m_N \sim 1$ GeV, this implies $m_\Sigma / y_N^2 \sim (v_\zeta/\text{GeV})^2 (1.2 \times 10^8\ \text{GeV})$.

We now turn to probe $\zeta^{\pm\pm}$ at the LHC. The sole method of producing the heavy Higgs quadruplet $\zeta^{\pm\pm}$ at the LHC through proton-proton collisions is by generating a pair of $\zeta^{\pm\pm}$ particles. This can occur through three specific mediators; via SM Higgs boson, photon, and Z-boson interactions, represented as $pp \to h/\gamma/z \to \zeta^{++}\zeta^{--}$. The combined cross section for these processes amounts to 8.6 fb. The ζ^{--} decay occurs through various channels, such as $\zeta^{--} \to W^-W^-, \zeta^-\zeta^-, W^-\zeta^-$, and $\Sigma^{--}N$. In our benchmark points, the masses of Σ^{--} and ζ^- exceed that of ζ^{--}. Hence, the most favorable decay pathway for ζ^{--} is to W^-W^-, with a decay rate of 0.16 fb. However. the exclusive decay of the doubly charged Higgs boson into same-sign W bosons is not exclusively tied to this specific model. It is also a characteristic feature of the Higgs triplet model within the type-II seesaw framework [58–61].

In our analysis, we consider an integrated luminosity of $L_{\text{int}} = 3000\ \text{fb}^{-1}$ at the center-of-mass energy of

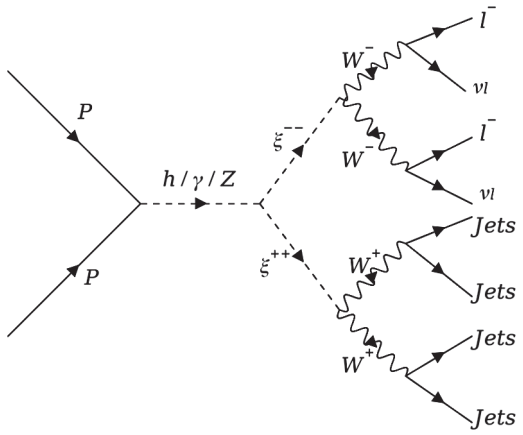

FIG. 4. Feynman diagram for the process $pp \to \zeta^{++}\zeta^{--} \to 2W^+2W^- \to 4j2l^- + \text{MET}$.

TABLE I. Cut-flow charts for the signal versus its relevant background and the corresponding number of events and significance.

Cuts (select)	Signal (S); $m_{\zeta^{\pm\pm}} = 400(500)$ GeV	Backgrounds ($\sum B$)	$S/\sqrt{B}$
Initial (no cut)	1620.0 (272.0)	459213.0	2.4 (0.4)
$H_T > 250.0$ GeV	1619.8 (272.0)	65102.0	6.4 (1.7)
$\not{H}_T > 400.0$ GeV	632.1 (143.0)	958.0	20.8 (4.7)
$(\Delta R)_{l^-l^-} > 0.5$	393.9 (85.4)	465.2	18.2 (4.3)
$\beta_{l^-l^-} > 0.75$	361.8 (73.1)	232.4	23.8 (5.4)
$M_T > 100.0$ GeV	241.1 (57.9)	102.6	23.9 (5.9)
$P_{l^-l^-} < 550.0$ GeV	202.4 (34.0)	55.6	27.6 (4.6)
$\phi_{l^-l^-} > 0.0$	101.9 (17.4)	5.1	44.7 (7.7)

$\sqrt{s} = 14$ TeV. To probe $\zeta^{\pm\pm}$, we explore the process $pp \to \zeta^{++}\zeta^{--} \to 2W^+2W^- \to 4j2l^- +$ missing energy (MET), depicted by the Feynman diagram in Fig. 4. We employ two benchmark points; one with $m_{\zeta_{\pm\pm}} = 400$ GeV and a total cross section of 0.14 fb, and another with $m_{\zeta_{\pm\pm}} = 500$ GeV and a total cross section of 0.05 fb. To detect $\zeta^{\pm\pm}$ at the LHC, we examine the signal alongside the corresponding background arising from SM processes. The primary background processes interfering with our signal are $pp \to WZ \to l^+ + 2l^- + \text{MET}$, $pp \to WWZ \to 2\,\text{jets} + l^+ + 2l^- + \text{MET}$, and $pp \to WWW \to 2\,\text{jets} + 2l^- + \text{MET}$.

Our strategy to eliminate these backgrounds involves plotting various kinematic distributions for the signal versus the backgrounds. These include parameters like Missing Transverse Energy ($\not{E}_T$), Missing transverse energy defined from the jet activity only ($\not{H}_T$), Scalar Sum of the Transverse Energy (H_T), scalar sum of the transverse energy of all final-state objects/jets (E_T/H_T), absolute value of the pseudorapidity ($|\eta|$), velocity (β), transverse energy ($E_{T_{l^-l^-}}$), magnitude of the three-momentum (P), angular distance in the transverse plane between objects (Δ_R), among others. We strategically select cuts that effectively suppress the background while preserving our signal. Table I presents the comprehensive list of all cuts employed to eliminate the backgrounds.

The concluding distributions of these events are depicted in Fig. 5, showcasing the invariant mass distribution for two same-sign leptons both pre and post the application of the cuts. A notable observation is that following the implementation of cuts, the signal exhibits a higher count of events compared to the background. We also explore another scenario to probe $\zeta^{\pm\pm}$ via the process $pp \to \zeta^{++}\zeta^{--} \to 2W^+2W^- \to 4l(l = e, \mu) +$ MET. However, in this scenario, the cross sections for masses of 400 and 500 GeV are notably small, amounting to 0.016(0.0056) fb for $m_{\zeta^{\pm\pm}} = 400\,(500)$ GeV. These extremely low cross sections (in fractions of fb) result in an exceedingly small number of events compared to the relevant background.

The work of K. E. and S. K. is partially supported by Science, Technology and Innovation Funding Authority (STDF) under Grant No. 48173. The work of E. M. is supported in part by the U.S. Department of Energy Grant No. DE-SC0008541. The work of D. N. is supported by the National Research Foundation of Korea (NRF)'s Grant No. 2019R1A2C3005009. D. N. also acknowledges Debasish Borah and Sanjoy Mandal for useful discussions.

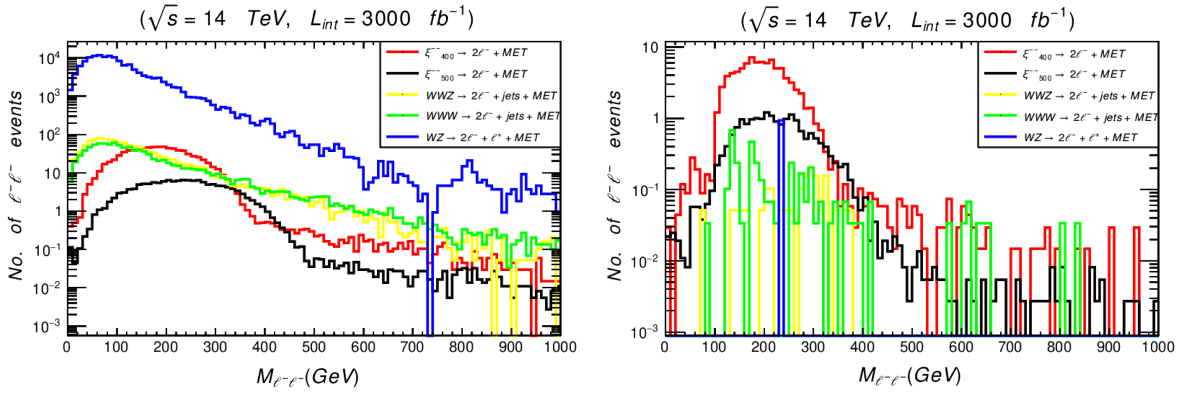

FIG. 5. Number of signal events for the process at mass $m_{\zeta^{\pm\pm}} = 400(500)$ GeV [red(black)], alongside the relevant background events background (yellow/green/blue) before (left) and after (right).

[1] T. Aaltonen *et al.* (CDF Collaboration), Science **376**, 170 (2022).
[2] R. L. Workman *et al.* (Particle Data Group), Prog. Theor. Exp. Phys. **2022**, 083C01 (2022).
[3] Y. Liao, J. High Energy Phys. 06 (2011) 098.
[4] K. Kumericki, I. Picek, and B. Radovcic, Phys. Rev. D **86**, 013006 (2012).
[5] R. Foot, H. Lew, X. G. He, and G. C. Joshi, Z. Phys. C **44**, 441 (1989).
[6] E. Ma, Phys. Rev. Lett. **81**, 1171 (1998).
[7] E. Ma, Phys. Rev. Lett. **86**, 2502 (2001).
[8] J. de Blas, M. Pierini, L. Reina, and L. Silvestrini, Phys. Rev. Lett. **129**, 271801 (2022).
[9] A. Strumia, J. High Energy Phys. 08 (2022) 248.
[10] P. Asadi, C. Cesarotti, K. Fraser, S. Homiller, and A. Parikh, Phys. Rev. D **108**, 055026 (2023).
[11] C.-T. Lu, L. Wu, Y. Wu, and B. Zhu, Phys. Rev. D **106**, 035034 (2022).
[12] Y.-Z. Fan, T.-P. Tang, Y.-L. S. Tsai, and L. Wu, Phys. Rev. Lett. **129**, 091802 (2022).
[13] C.-R. Zhu, M.-Y. Cui, Z.-Q. Xia, Z.-H. Yu, X. Huang, Q. Yuan, and Y.-Z. Fan, Phys. Rev. Lett. **129**, 231101 (2022).
[14] B.-Y. Zhu, S. Li, J.-G. Cheng, X.-S. Hu, R.-L. Li, and Y.-F. Liang, Phys. Rev. D **108**, 083034 (2023).
[15] J. Kawamura, S. Okawa, and Y. Omura, Phys. Rev. D **106**, 015005 (2022).
[16] K. I. Nagao, T. Nomura, and H. Okada, Eur. Phys. J. Plus **138**, 365 (2023).
[17] X. Liu, S.-Y. Guo, B. Zhu, and Y. Li, Sci. Bull. **67**, 1437 (2022).
[18] T.-K. Chen, C.-W. Chiang, and K. Yagyu, Phys. Rev. D **106**, 055035 (2022).
[19] K. Sakurai, F. Takahashi, and W. Yin, Phys. Lett. B **833**, 137324 (2022).
[20] G. Cacciapaglia and F. Sannino, Phys. Lett. B **832**, 137232 (2022).
[21] H. Song, W. Su, and M. Zhang, J. High Energy Phys. 10 (2022) 048.
[22] H. Bahl, J. Braathen, and G. Weiglein, Phys. Lett. B **833**, 137295 (2022).
[23] Y. Cheng, X.-G. He, Z.-L. Huang, and M.-W. Li, Phys. Lett. B **831**, 137218 (2022).
[24] K. S. Babu, S. Jana, and P. K. Vishnu, Phys. Rev. Lett. **129**, 121803 (2022).
[25] Y. Heo, D.-W. Jung, and J. S. Lee, Phys. Lett. B **833**, 137274 (2022).
[26] Y. H. Ahn, S. K. Kang, and R. Ramos, Phys. Rev. D **106**, 055038 (2022).
[27] M.-D. Zheng, F.-Z. Chen, and H.-H. Zhang, AAPPS Bull. **33**, 16 (2023).
[28] P. Fileviez Perez, H. H. Patel, and A. D. Plascencia, Phys. Lett. B **833**, 137371 (2022).
[29] S. Kanemura and K. Yagyu, Phys. Lett. B **831**, 137217 (2022).
[30] J. Fan, L. Li, T. Liu, and K.-F. Lyu, Phys. Rev. D **106**, 073010 (2022).
[31] E. Bagnaschi, J. Ellis, M. Madigan, K. Mimasu, V. Sanz, and T. You, J. High Energy Phys. 08 (2022) 308.
[32] X. K. Du, Z. Li, F. Wang, and Y. K. Zhang, Nucl. Phys. **B989**, 116151 (2023).
[33] T.-P. Tang, M. Abdughani, L. Feng, Y.-L. S. Tsai, J. Wu, and Y.-Z. Fan, Sci. China Phys. Mech. Astron. **66**, 239512 (2023).
[34] J. M. Yang and Y. Zhang, Sci. Bull. **67**, 1430 (2022).
[35] P. Athron, M. Bach, D. H. J. Jacob, W. Kotlarski, D. Stöckinger, and A. Voigt, Phys. Rev. D **106**, 095023 (2022).
[36] A. Ghoshal, N. Okada, S. Okada, D. Raut, Q. Shafi, and A. Thapa, Nucl. Phys. **B989**, 116099 (2023).
[37] G.-W. Yuan, L. Zu, L. Feng, Y.-F. Cai, and Y.-Z. Fan, Sci. China Phys. Mech. Astron. **65**, 129512 (2022).
[38] P. Athron, A. Fowlie, C.-T. Lu, L. Wu, Y. Wu, and B. Zhu, Nat. Commun. **14**, 659 (2023).
[39] M. Blennow, P. Coloma, E. Fernández-Martínez, and M. González-López, Phys. Rev. D **106**, 073005 (2022).
[40] J. J. Heckman, Phys. Lett. B **833**, 137387 (2022).
[41] H. M. Lee and K. Yamashita, Eur. Phys. J. C **82**, 661 (2022).
[42] L. Di Luzio, R. Gröber, and P. Paradisi, Phys. Lett. B **832**, 137250 (2022).
[43] A. Paul and M. Valli, Phys. Rev. D **106**, 013008 (2022).
[44] T. Biekötter, S. Heinemeyer, and G. Weiglein, Eur. Phys. J. C **83**, 450 (2023).
[45] R. Balkin, E. Madge, T. Menzo, G. Perez, Y. Soreq, and J. Zupan, J. High Energy Phys. 05 (2022) 133.
[46] K. Cheung, W.-Y. Keung, and P.-Y. Tseng, Phys. Rev. D **106**, 015029 (2022).
[47] X. K. Du, Z. Li, F. Wang, and Y. K. Zhang, Eur. Phys. J. C **83**, 139 (2023).
[48] M. Endo and S. Mishima, Phys. Rev. D **106**, 115005 (2022).
[49] A. Crivellin, M. Kirk, T. Kitahara, and F. Mescia, Phys. Rev. D **106**, L031704 (2022).
[50] F. Arias-Aragón, E. Fernández-Martínez, M. González-López, and L. Merlo, J. High Energy Phys. 09 (2022) 210.
[51] M. E. Peskin and T. Takeuchi, Phys. Rev. Lett. **65**, 964 (1990).
[52] M. E. Peskin and T. Takeuchi, Phys. Rev. D **46**, 381 (1992).
[53] K. S. Kumar, S. Mantry, W. J. Marciano, and P. A. Souder, Annu. Rev. Nucl. Part. Sci. **63**, 237 (2013).
[54] S. Dawson and C. W. Murphy, Phys. Rev. D **96**, 015041 (2017).
[55] C. W. Murphy, J. High Energy Phys. 10 (2020) 174.
[56] E. Ma and V. De Romeri, Phys. Rev. D **104**, 055004 (2021).
[57] G. Arcadi and L. Covi, J. Cosmol. Astropart. Phys. 08 (2013) 005.
[58] C.-W. Chiang, T. Nomura, and K. Tsumura, Phys. Rev. D **85**, 095023 (2012).
[59] S. Kanemura, M. Kikuchi, K. Yagyu, and H. Yokoya, Phys. Rev. D **90**, 115018 (2014).
[60] A. Melfo, M. Nemevsek, F. Nesti, G. Senjanovic, and Y. Zhang, Phys. Rev. D **85**, 055018 (2012).
[61] S. Ashanujjaman and K. Ghosh, J. High Energy Phys. 03 (2022) 195.